Measurement of the proton-air inelastic cross section at $\sqrt{s} \approx 2$ TeV from the EAS-TOP experiment

M. Aglietta,[1,2] B. Alessandro,[2] P. Antonioli,[3] F. Arneodo,[4] L. Bergamasco,[2,5] M. Bertaina,[2,5] A. Castellina,[1,2] E. Cantoni,[1,5] A. Chiavassa,[2,5] B. D'Ettorre Piazzoli,[6] G. Di Sciascio,[6,*] W. Fulgione,[1,2] P. Galeotti,[2,5] P. L. Ghia,[1,†] M. Iacovacci,[6] G. Mannocchi,[1,2] C. Morello,[1,2] G. Navarra,[2,5] O. Saavedra,[2,5] A. Stamerra,[5,‡] G. C. Trinchero,[1,2] P. Vallania,[1,2] S. Vernetto,[1,2] and C. Vigorito[2,5]

(EAS-TOP Collaboration)

[1]*Istituto di Fisica dello Spazio Interplanetario (INAF), I-10133 Torino, Italy*
[2]*Istituto Nazionale di Fisica Nucleare, I-10125 Torino, Italy*
[3]*Istituto Nazionale di Fisica Nucleare, I-40126 Bologna, Italy*
[4]*Laboratori Nazionali del Gran Sasso, INFN, I-67010 Assergi (AQ), Italy*
[5]*Dipartimento di Fisica Generale dell'Università, I-10125 Torino, Italy*
[6]*Dipartimento di Scienze Fisiche dell'Università and INFN, I-80126 Napoli, Italy*

(Received 1 December 2008; published 23 February 2009)

The proton-air inelastic cross section ($\sigma^{\text{inel}}_{p\text{-air}}$) is measured at $\sqrt{s} \approx 2$ TeV at the EAS-TOP extensive air shower experiment by studying the absorption length of cosmic ray proton primaries cascades reaching the maximum development at the observation level. Primary energies, in the region $E_0 = (1.5 \div 2.5) \cdot 10^{15}$ eV, are selected through the EAS muon number (N_μ), and proton originated cascades at maximum development are selected by means of the shower size (N_e). The observed absorption length (λ_{obs}) is a convolution of the proton-air interaction length ($\lambda_{p\text{-air}}$) and of the shower and detector fluctuations. The conversion factor $k = \lambda_{\text{obs}}/\lambda_{\text{int}}$ is obtained by means of simulations performed with the CORSIKA code and the QGSJET II and SIBYLL interaction models. The obtained value of the p-air inelastic cross section at $\sqrt{s} \approx 2$ TeV is $\sigma^{\text{inel}}_{p\text{-air}} = 338 \pm 21(\text{stat}) \pm 19(\text{syst}) - 28(\text{syst})$ mb. The statistical and systematic uncertainties, as well as the relationships with the pp ($\bar{p}p$) total cross section measurements are discussed.

DOI: 10.1103/PhysRevD.79.032004 PACS numbers: 13.85.Tp, 96.50.sd

I. INTRODUCTION

Hadronic cross section measurements at energies above the accelerators' limits have to be performed by exploiting the cosmic ray beam. This holds, in particular, for nucleus-nucleus interactions as the typical p-N and p-O (''p-air'') ones, which determine the development of extensive air showers (EAS). The most relevant datum to which the EAS development is sensitive is the p-air inelastic cross section ($\sigma^{\text{inel}}_{p\text{-air}}$). In this work we will address its measurement. We will focus on primary energies $\sqrt{s} \approx 2$ TeV, which are of particular interest for both high energy physics and astrophysics issues:

(i) The pp total cross section, σ^{tot}_{pp}, and the proton-air inelastic cross section $\sigma^{\text{inel}}_{p\text{-air}}$ are related and can be inferred one from each other by means of the Glauber theory [1]. The whole procedure is model dependent, the results [2–9] differing by about 20% for $\sqrt{s}$ values in the TeV energy range. It is therefore of primary interest to have experimental measurements of $\sigma^{\text{inel}}_{p\text{-air}}$ and σ^{tot}_{pp} at the same center of mass (CM) energy, i.e. around $\sqrt{s} \approx 2$ TeV, at which collider data are still available.

(ii) At the highest energies, the direct accelerator measurements themselves can be affected by systematic uncertainties of difficult evaluation, and, as a matter of fact, the available pp ($\bar{p}p$) cross section data at energies of $\sqrt{s} = 1.8$ TeV differ by about 10%, which exceeds the statistical uncertainties of the individual measurements [10–12] introducing further indetermination in the p-nucleus cross section.

(iii) From the point of view of cosmic ray physics, the interpretation of extensive air shower measurements (e.g. concerning primary energy and composition studies) rely on simulations based on hadronic interaction models. Such models are based on theoretically guided extrapolations of the accelerator data obtained at lower energies (and usually restricted to limited kinematical regions). A direct measurement of $\sigma^{\text{inel}}_{p\text{-air}}$ and the comparison of basic quantities as obtained from measurements and model based simulations, in the same conditions, is therefore of primary relevance for the validation of the methodology. This can be best performed at primary

*Present address: Istituto Nazionale di Fisica Nucleare, Tor Vergata, I-00133 Roma, Italy.
†Present address: Institut de Physique Nucleaire, CNRS, 91406 Orsay, France.
‡Present address: Dipartimento di Fisica dell'Università and INFN, I-56127 Pisa, Italy.

energies below the steepening (*knee*) of the primary spectrum (i.e. $E_0 < 3.10^{15}$ eV, $\sqrt{s} < 2.5$ TeV) above which the proton flux is strongly reduced [13–15].

Measurements of the p-air inelastic cross section performed in EAS have been reported. Since air shower detectors cannot observe the depth of the first interaction of the primary particle, they are based on the study of the fluctuations of the cascades' maximum development. Two main techniques are exploited: the constant N_e-N_μ cuts [16–18] by means of particle arrays, and the study of the shower profiles using fluorescence detectors [19,20] above 10^{17} eV.

Following the particle array technique, the primary energy is first selected by means of the muon number (N_μ). Proton induced showers at maximum development are then selected by means of the shower size (dominated by the electron number N_e). The cross section of primary particles is obtained by studying the absorption in the atmosphere ($\lambda_{\rm obs}$) of such showers, through their angular distribution at the observation level. Moreover the observed absorption length is affected by the fluctuations in the longitudinal development of the cascades and in the detector response. Such fluctuations can be studied through simulations, providing the conversion factor k between the observed absorption length and the interaction length of primary protons ($k = \lambda_{\rm obs}/\lambda_{\rm int}$).

The N_e-N_μ method has been exploited by EAS-TOP [18] at primary energy $E_0 \approx 2 \cdot 10^{15}$ eV (i.e. $\sqrt{s} \approx 2$ TeV). We present the analysis of the complete data set (a total of $1.5 \cdot 10^7$ events collected between 1997 and 1999, for an effective uptime of 7600 hours) based on the most up to date hadronic interaction models.

Systematic uncertainties of the measurement and the effect of possible contaminations from heavier primaries are discussed and evaluated.

II. THE EXPERIMENT AND THE SIMULATION

The EAS-TOP array was located at Campo Imperatore, Gran Sasso National Laboratory, 2005 m above sea level, 820 g/cm^2 atmospheric depth.

The electromagnetic (e.m.) detector consisted of 35 modules 10 m^2 each of plastic scintillators, 4 cm thick, distributed over an area of 10^5 m^2. For this analysis, only events with at least six modules fired in a compact configuration, and the largest number of particles recorded by a module inside the edges of the array are selected. Such triggering condition is fully efficient for $N_e > 10^5$, i.e. for primary proton energies $E_0 > 3 \cdot 10^{14}$ eV. Core location (X_c, Y_c), shower size (N_e), and slope of the lateral distribution function (s) are obtained by fitting the recorded number of particles in each module with the Nishimura-Kamata-Greisen (NKG) expression [21]. The experimental resolutions for $N_e > 2 \cdot 10^5$ are $\sigma_{N_e}/N_e \simeq 0.1$; $\sigma_{X_c} = \sigma_{Y_c} \simeq 5$ m; $\sigma_s \simeq 0.1$. The arrival direction of the shower is measured from the times of flight among the modules with resolution $\sigma_\theta \simeq 0.9°$. A detailed description of the performance of the e.m. detector can be found in Ref. [22].

The muon-hadron detector (MHD), located at one edge of the e.m. array, is used, for the present analysis, as a tracking module with 9 active planes. Each plane includes two layers of streamer tubes (12 m length, 3×3 cm^2 section) and is shielded by 13 cm of iron. The total height of the detector is 280 cm and the surface is 12×12 m^2. A muon track is defined by the alignment of at least 6 fired wires in different streamer tube layers leading to an energy threshold of $E_\mu^{\rm th} \approx 1$ GeV.

The accuracy of the muon reconstruction depends on the muon number: for $N_\mu \approx 15$, 70% of the events are inside $\Delta N_\mu^{70\%} = \pm 1$ ($\Delta N_\mu^{70\%} = \pm 2$ for $N_\mu \approx 30$). The tails of the error distribution are rather limited: e.g. the rate of large errors, exceeding 50% of the muon number, is of 0.1%. The muon number, and therefore its uncertainty, depends on primary energy, core distance and zenith angle. For this reason, events were selected in order to fulfil the quoted reconstruction accuracy of the tracking detector. The applied selection in core distance and zenith angle (''$r - \theta$'' selection: 50 m $< r <$ 100 m, and maximum zenith angle $\theta_{\rm max} = 33.6°$) provides a number of muons ranging from 6 to 23 in our energy region [see (a) in Sec. III]. This guarantees that the muon counting uncertainties are always dominated by Poissonian fluctuations. The total number of events that pass this selection is $1.7 \cdot 10^6$.

EAS simulations are performed utilizing the CORSIKA program [23] with QGSJET II.03 and SIBYLL 2.1 high energy hadronic interaction models [24,25]. These models have been widely employed for simulating atmospheric shower developments and have been shown to provide consistent descriptions of different shower parameters in the considered energy range. Hadrons with energies below 80 GeV are treated with the GHEISHA 2002 [26] interaction model.

The shower size (N_e) is obtained by adding all contributions from the produced γ rays (mainly from π^0 decays) following Greisen expression [27], as provided by CORSIKA. The obtained N_e value at the observation level is distributed over the e.m. modules following the NKG lateral distribution function (ldf) [21], with slopes (s) sampled from the experimental data [13]. The effect of using the standard NKG ldf in real scintillator arrays has been discussed in Refs. [13,28], where it has been shown that the deviation results are lower than 3% for proton showers with $N_e \approx 10^6$ up to 150 m from the core. The conversion from the zero energy threshold N_e value obtained from Greisen formula to the experimental N_e value measured (as usual) in minimum ionizing particle (mip) units ($N_{e,\rm mip}$) has been obtained by means of simulations of e.m. showers in the atmosphere, in the scintillators and their housings, based on the GEANT [29] code. It has been

further verified by means of a test performed with the same scintillators and electronics operating in the field, at the CERN SPS with positron beams up to $E_{e^+} = 50$ GeV. The relation between N_e and $N_{e,\mathrm{mip}}$ is $N_e = N_{e,\mathrm{mip}}/1.18$ for zenith angles up to 40° [13]. The muon contribution to N_e is added in the individual e.m. units (its overall contribution being lower than 5%). Poissonian fluctuations and parameterized expressions of experimental uncertainties have been included, as well as trigger requirements.

The full response of the muon detector is included by means of simulations based on the GEANT code taking into account the measured experimental efficiencies of the streamer tubes. Simulated events have been treated using the same procedure followed for experimental data.

Proton showers have been simulated with an energy threshold of 10^{15} eV, spectral index $\gamma = 2.7$ (from which KASCADE spectra [15] have been afterward sampled[1]), and uniform angular distribution. Every shower has been sampled over an area of $4.4 \cdot 10^5$ m^2 until the event fulfills the "$r - \theta$" and trigger requirements. The number of trials ($n_T(\theta)$) is recorded and then used to calculate the angular acceptance.

III. THE METHOD AND THE ANALYSIS

The rate of showers of given primary energy ($E_{0,1} < E_0 < E_{0,2}$) selected through their muon number N_μ ($N_{\mu,1} < N_\mu < N_{\mu,2}$) and shower size N_e corresponding to maximum development ($N_{e,1} < N_e < N_{e,2}$) is expected to decrease exponentially with atmospheric depth. This can be expressed as a function of the zenith angle θ by the equation

$$f(\theta) = G(\theta) f(0) \exp[-x_0(\sec\theta - 1)/\lambda_{\mathrm{obs}}], \qquad (1)$$

where x_0 is the vertical atmospheric depth of the detector, and $G(\theta)$ the angular acceptance.

The observed absorption length λ_{obs}, obtained from (1), is a combination of the interaction mean free path (λ_{int}), and of the shower development and detector response fluctuations. Fluctuation effects are evaluated through simulations, by comparing $\lambda_{\mathrm{obs}}^{\mathrm{sim}}$ (the observed absorption length obtained in simulations) and $\lambda_{\mathrm{int}}^{\mathrm{sim}}$ (the interaction length, which is known from the interaction model), and can be expressed by the factor $k = \lambda_{\mathrm{obs}}^{\mathrm{sim}}/\lambda_{\mathrm{int}}^{\mathrm{sim}}$. This factor is then used to convert the observed experimental absorption length $\lambda_{\mathrm{obs}}^{\mathrm{exp}}$ into the interaction one $\lambda_{\mathrm{int}}^{\mathrm{exp}}$.

The physical quantities required for the analysis are obtained through simulations, based on QGSJET II and SIBYLL interaction models, as described below.

(a) Events in the specific proton primary energy range $[E_0 = (1.5 \div 2.5) \cdot 10^{15}$ eV] are selected by means of a matrix of minimum ($N_{\mu,1}$) and maximum ($N_{\mu,2}$) detected muon numbers for every possible combination of zenith angle and core distance from the muon detector. The selection table is obtained from simulated data for 5 m bins in core distance (50 m $\leq r \leq$ 100 m) and 0.025 secθ bins ($1.0 \leq \sec\theta \leq 1.2$) for zenith angle. $N_{\mu,1}$ and $N_{\mu,2}$ correspond to the average muon number recorded in the MHD, respectively, for $E_0 = 1.5 \cdot 10^{15}$ eV and $E_0 = 2.5 \cdot 10^{15}$ eV. $N_{\mu,1}$ ranges from 6 ($\sec\theta = 1.2$, $r =$ 100 m) to 15 ($\sec\theta = 1.0$, $r = 50$ m) and $N_{\mu,2}$ from 8 to 23.

(b) The selection of proton initiated cascades near maximum development is based on simulated distributions of the shower sizes at maximum development $N_e^{\max}$ in the selected energy interval.
The distribution calculated with QGSJET II is shown in Fig. 1. Choosing the shower size interval $\overline{\mathrm{Log}N_e^{\max}} \pm \sigma_{\mathrm{Log}N_e^{\max}}$ (i.e. $6.01 < \mathrm{Log}N_e < 6.17$ for both interaction models) provides the selection of about 65% of the events around the maximum of the distribution.
The fraction of simulated events (QGSJET II proton primaries) accepted after the muon cut is 26%, over them 5% passing the N_e selection (averaged over all zenith angles) for a total of 8885 events. The corresponding fractions of experimental events are, respectively, 18.5% and 0.5% for a total of 1384 events. The experimental fraction of events passing

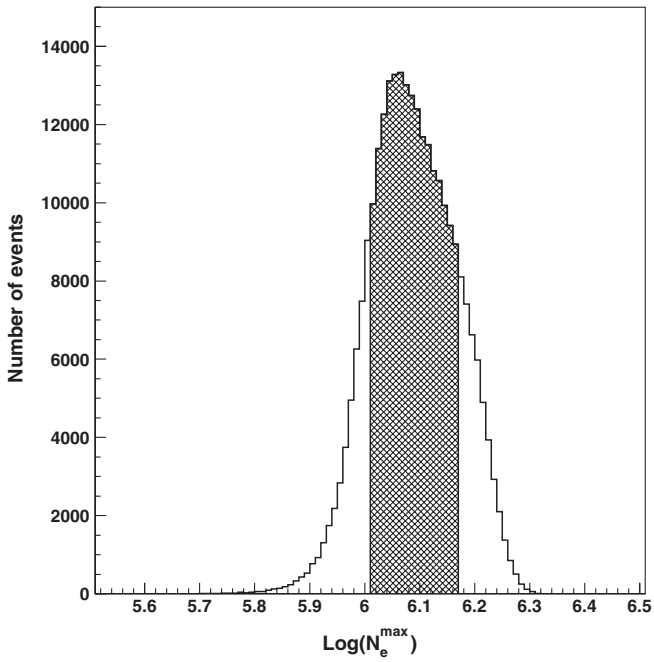

FIG. 1. Shower size distribution at maximum development ($N_e^{\max}$) for proton showers simulated with QGSJET II in the selected energy range $[E_0 = (1.5 \div 2.5) \cdot 10^{15}$ eV]. The shaded area represents the N_e interval considered in the analysis.

[1]The power law indexes of proton and helium spectra (resulting from our own fits) are, respectively, $\gamma_{p,1}(E_0 < 2 \cdot 10^{15}$ eV$) = 2.6$, $\gamma_{p,2}(2 \cdot 10^{15}$ eV$ < E_0 < 4.5 \cdot 10^{15}$ eV$) = 3.3$, $\gamma_{p,3}(E_0 > 4.5 \cdot 10^{15}$ eV$) = 5.0$ and $\gamma_{\mathrm{He}} = 2.65$.

the N_e selection is lower than in simulation, due to the contribution of heavy primaries.

The effective energy distribution of the selected primaries is shown in Fig. 2, the median value being $E_0^{\text{median}} = 2.49 \cdot 10^{15}$ eV with rms $0.78 \cdot 10^{15}$ eV and $E_0^{\text{median}} = 2.50 \cdot 10^{15}$ eV with rms $0.80 \cdot 10^{15}$ eV for QGSJET II and SIBYLL, respectively.

(c) For simulated data, due to the imposed full detection efficiency, the acceptance $G(\theta)$ in each individual $\sec\theta$ bin ($1.0 \leq \sec\theta \leq 1.2$, $\Delta \sec\theta = 0.05$) is simply given by the geometrical acceptance $G_1(\theta)$. For experimental data, in order to take into account the "$r - \theta$" acceptance, $G_1(\theta)$ is further multiplied by the number of trials performed in order to accept the primaries generated following the input uniform distribution $[G(\theta) = G_1(\theta) \cdot n_T(\theta)/n_T(0)]$. Therefore, the number of events (corrected for acceptance effects) in each $\sec(\theta)$ bin is $N'_{\text{sel}} = N_{\text{sel}} \cdot G(\theta)$.

(d) The interaction length $\lambda_{\text{int}}^{\text{sim}}$ is obtained as the average proton interaction depth in the selected energy range $[E_0 = (1.5 \div 2.5) \cdot 10^{15}$ eV], and results to be $\lambda_{\text{int}}^{\text{sim}} = 60.3 \pm 0.1$ g/cm^2 for QGSJET II and $\lambda_{\text{int}}^{\text{sim}} = 59.4 \pm 0.1$ g/cm^2 for SIBYLL.

The acceptance corrected numbers of selected events vs zenith angle are shown in Fig. 3. The fit with expression (1) provides $\lambda_{\text{obs}}^{\text{sim}} = 68.5 \pm 1.4$ g/cm^2 for QGSJET II and $\lambda_{\text{obs}}^{\text{sim}} = 69.9 \pm 1.4$ g/cm^2 for SIBYLL. Therefore $k = \lambda_{\text{obs}}^{\text{sim}}/\lambda_{\text{int}}^{\text{sim}} = 1.14 \pm 0.02$ for QGSJET II and $k = 1.18 \pm 0.02$ for SIBYLL (see Table I).

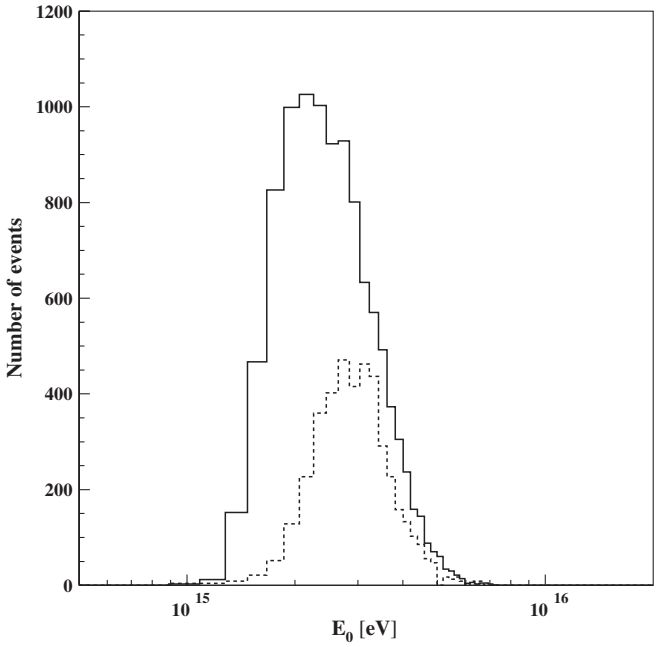

FIG. 2. Primary energy distribution of simulated proton events selected with the N_μ-N_e cuts (continuous line). The energy distribution of helium primaries satisfying the same selection criteria is also shown (dashed line).

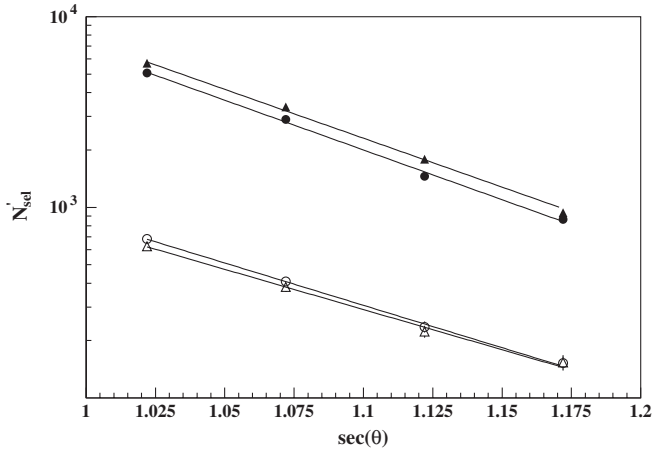

FIG. 3. Acceptance corrected number of events vs $\sec\theta$ for the simulated (solid circle for QGSJET II and solid triangle for SIBYLL) and experimental data selected with the N_μ-N_e cuts calculated with the two interaction models (open circle for QGSJET II and open triangle for SIBYLL). The fits with expression (1) providing the λ_{obs} values are also shown (continuous lines).

IV. SYSTEMATIC UNCERTAINTIES

The data obtained from simulations with different interaction models, characterized by different cross sections, have been used in order to evaluate the systematic uncertainties of the analysis, as described in the following.

(i) The analysis procedure based on one interaction model has been applied to a simulated experimental data set produced with a different interaction model with known p-air inelastic cross section (i.e. experimental data simulated with SIBYLL are analyzed with QGSJET II and vice versa).

(ii) An experimental data set has been simulated using QGSJET II with a cross section value about 10% lower in order to check the capability to discriminate between two different values of the p-air cross section within the same interaction model. The lower cross section of the HDPM interaction model [30] has been utilized. The two data sets are analyzed using the parameters established with SIBYLL.

The results of these analyses are reported in Table II, from which we can note the following:

(a) Differences from the simulated $\sigma_{p\text{-air}}^{\text{inel}}$ values are both positive and negative implying that there is no systematic underestimation or overestimation.

(b) The analysis performed with SIBYLL clearly discriminate between the two different values of $\sigma_{p\text{-air}}^{\text{inel}}$ used in the simulations with QGSJET II.

(c) The four differences between the simulated and measured values ($\Delta\sigma_{p\text{-air}}^{\text{inel}}$) are compatible with the statistical uncertainties.

Therefore we define as maximum systematic uncertainty the value $\sigma_{\text{syst}} = 19$ mb which provides the χ^2 value cor-

TABLE I. Summary of the results obtained with different high energy interaction models. The interaction length $\lambda_{\rm int}^{\rm sim}$ is the average proton interaction depth in the selected energy range. $\lambda_{\rm obs}^{\rm sim}$ and $\lambda_{\rm obs}^{\rm exp}$ are obtained, respectively, from the fits of the simulated and experimental distribution of event rates vs zenith angle as shown in Fig. 3. The factor $k = \lambda_{\rm obs}^{\rm sim}/\lambda_{\rm int}^{\rm sim}$ accounts for fluctuations in longitudinal shower development and detector response.

High energy hadronic interaction model	$\lambda_{\rm int}^{\rm sim}$ [g/cm^2]	$\lambda_{\rm obs}^{\rm sim}$ [g/cm^2]	k	$\lambda_{\rm obs}^{\rm exp}$ [g/cm^2]	$\lambda_{\rm int}^{\rm exp}$ [g/cm^2]	$\sigma_{p\text{-air}}^{\rm inel}$ [mb]
SIBYLL 2.1	59.4 ± 0.1	69.9 ± 1.4	1.18 ± 0.02	84.7 ± 5.0	71.8 ± 4.5	336 ± 21
QGSJET II	60.3 ± 0.1	68.5 ± 1.4	1.14 ± 0.02	80.2 ± 4.3	70.7 ± 4.2	341 ± 20

TABLE II. Proton-air inelastic cross section values ($\sigma_{p\text{-air}}^{\rm inel}$) obtained using the simulated data sets as "experimental" ones in order to determine the observed experimental absorption length ($\lambda_{\rm obs}^{\rm exp}$). Results of the analyses with the two interaction models are reported. The intrinsic $\sigma_{p\text{-air}}^{\rm inel}$ of each model and the differences from measured values ($\Delta\sigma_{p\text{-air}}^{\rm inel}$) are also reported.

Experiment	SIBYLL 2.1 ($\sigma_{p\text{-air}}^{\rm inel} = 406 \pm 1$ mb)		QGSJET II ($\sigma_{p\text{-air}}^{\rm inel} = 400 \pm 1$ mb)		QGSJET II$_{\rm HDPM}$ ($\sigma_{p\text{-air}}^{\rm inel} = 367 \pm 1$ mb)	
Analysis	$\sigma_{p\text{-air}}^{\rm inel}$ [mb]	$\Delta\sigma_{p\text{-air}}^{\rm inel}$ [mb]	$\sigma_{p\text{-air}}^{\rm inel}$ [mb]	$\Delta\sigma_{p\text{-air}}^{\rm inel}$) [mb]	$\sigma_{p\text{-air}}^{\rm inel}$ [mb]	$\Delta\sigma_{p\text{-air}}^{\rm inel}$ [mb]
SIBYLL 2.1	…	…	419 ± 12	$+19 \pm 12$	372 ± 13	$+5 \pm 13$
QGSJET II	393 ± 11	-13 ± 11	…	…	361 ± 12	-6 ± 12

responding to 99% C.L. for the distribution of the four deviations $\Delta\sigma_{p\text{-air}}^{\rm inel}$.

V. RESULTS

The same analysis procedure discussed for the simulations is applied to the experimental data. The corresponding event numbers as a function of sec(θ) are shown in Fig. 3, together with their fit providing $\lambda_{obs}^{exp} = 80.2 \pm 4.3$ g/cm^2 and $\lambda_{obs}^{exp} = 84.7 \pm 5.0$ g/cm^2 for QGSJET II and SIBYLL, respectively. From the relation $\lambda_{\rm int}^{\rm exp} = \lambda_{\rm obs}^{\rm exp}/k$, we obtain $\lambda_{int}^{exp} = \lambda_{p-\rm air} = 70.7 \pm 4.2$ g/cm^2 for QGSJET II and $\lambda_{int}^{exp} = \lambda_{p-\rm air} = 71.8 \pm 4.5$ g/cm^2 for SIBYLL. The p-air inelastic cross section is then obtained from the relation $\sigma_{p-\rm air}^{\rm inel}$ (mb) $= 2.41 \cdot 10^4/\lambda_{p-\rm air}$, and results to be $\sigma_{p-\rm air}^{\rm inel} = 341 \pm 20$ mb with QGSJET II and $\sigma_{p-\rm air}^{\rm inel} = 336 \pm 21$ mb with SIBYLL analysis (see Table I). The given uncertainties are the statistical ones of both the measurement and the simulation. Therefore the two results, based on two different interaction models, are in excellent agreement.

The contribution of heavier nuclei has been evaluated by simulating helium primaries with QGSJET II, assuming the KASCADE spectrum and composition, which accounts for an He flux about twice that of the protons in the energy range of interest (see footnote 1 and Fig. 2). The overall simulated observed absorption length becomes $\lambda_{\rm obs}^{{\rm sim}(p+{\rm He})} = 62.6 \pm 1.0$ g/cm^2, which implies $k^{(p+{\rm He})} = 1.04 \pm 0.02$, and $\sigma_{p\text{-air}}^{\rm inel} = 312 \pm 17$ mb, decreased of about 8%. Because of the uncertainty of the relative proton/helium flux we will not introduce such correction, but rather consider it as a systematic uncertainty, possibly leading to an overestimated cross section value. Heavier primaries, such as CNO, hardly pass the N_μ-N_e cuts and result in an additional effect of less than 1%. Combining the results obtained with the two considered interaction models and including the systematic uncertainties discussed in the previous section, the p-air inelastic cross section is

$$\sigma_{p\text{-air}}^{\rm inel} = 338 \pm 21_{\rm stat} \pm 19_{\rm syst} - 29_{\rm syst(He)}\ {\rm mb}. \quad (2)$$

This value is plotted together with other experimental results and the cross sections within different hadronic interaction models in Fig. 4.

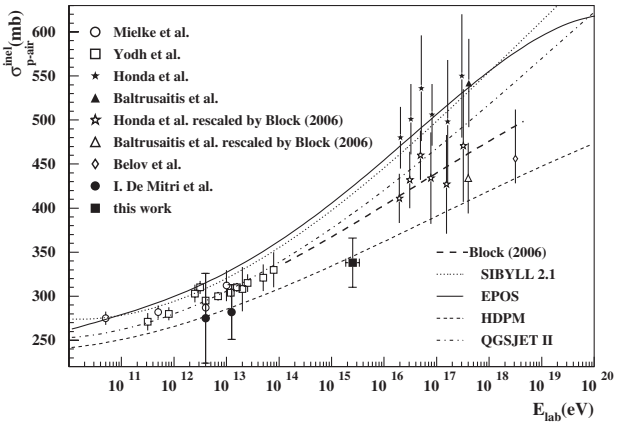

FIG. 4. p-air inelastic cross section data (open circle [32], open square [33], solid star [17], solid triangle [19], open star [8,17], open triangle [8,19], open diamond [20], solid circle [34]), including the present measurement (solid square), and values used by different hadronic interaction models (solid line [35], dotted line [25], dash-dotted line [24], dashed line [30]).

VI. CONCLUSIONS

The absorption length of cosmic ray proton showers at maximum development in the energy range $E_0 = (1.5 \div 2.5) \cdot 10^{15}$ eV (i.e. at $\sqrt{s} \approx 2$ TeV) is measured at the atmospheric depth of 820 g/cm^2.

Two independent analyses based on two different interaction models (QGSJET II and SIBYLL) have been exploited.

The experimental values of the p-air inelastic cross section at $\sqrt{s} \approx 2$ TeV are, respectively, $\sigma^{\text{inel}}_{p\text{-air}} = 341 \pm 20$ mb for QGSJET II and $\sigma^{\text{inel}}_{p\text{-air}} = 336 \pm 21$ mb for the SIBYLL analysis.

The contamination of heavier primaries (principally helium) has been evaluated resulting in a possible systematic effect that can lead to about an 8% overestimation of the p-air inelastic cross section.

The systematic uncertainties of the analysis procedure have been studied, and an upper limit has been obtained.

The experimental value of the p-air inelastic cross section obtained from the analysis of EAS-TOP data can be expressed as

$$\sigma^{\text{inel}}_{p\text{-air}} = 338 \pm 21_{\text{stat}} \pm 19_{\text{syst}} - 29_{\text{syst(He)}} \text{ mb}.$$

This value is about 20% smaller than the values in use within QGSJET II and SIBYLL and in better agreement with Refs. [8,30,31].

Predicted $\sigma^{\text{inel}}_{p\text{-air}}$ values, obtained from different σ^{tot}_{pp} Tevatron measurements at $\sqrt{s} = 1.8$ TeV by using different calculations based on the Glauber theory, are reported in Fig. 5. The present measurement is consistent with smaller values of the $\bar{p}p$ total cross section ($\sigma^{\text{tot}}_{pp} = 72.8 \pm 3.1$ mb [11], and $\sigma^{\text{tot}}_{pp} = 71 \pm 2$ mb [12]), and the pp to p-air calculations predicting for a given value of σ^{tot}_{pp}, a smaller value of $\sigma^{p\text{-air}}_{\text{in}}$ [8,9].

Independently from the cross section analysis, the measured value of the absorption length λ_{obs} can be directly compared with the analogous one obtained from simulations based on QGSJET II and SIBYLL. As shown in Table I, the experimental values are about 20% higher than the simulated ones for both the considered interaction models. This can be ascribed to a deeper shower penetration in the atmosphere with respect to the predictions of the interaction models, as reflected in the corresponding lower value of the p-air inelastic cross section.

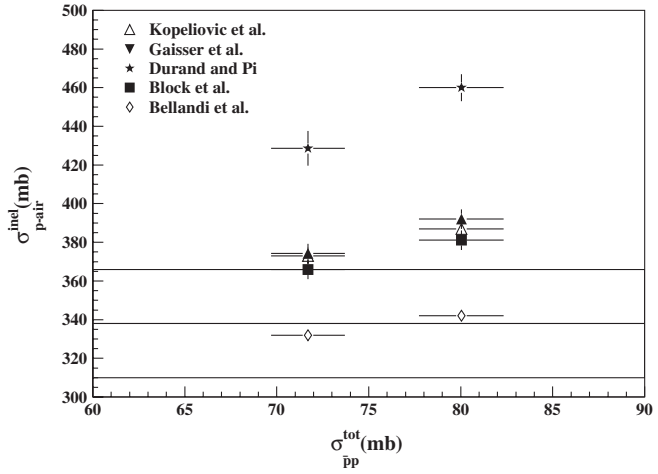

FIG. 5. p-air inelastic vs $\bar{p}p$ total cross section data. The present result (± 1 standard deviation, solid lines) is shown together with the results of different calculations (solid star [4], solid triangle [3], open triangle [5], solid square [8], open diamond [9]), derived from $\bar{p}p$ measurements reported at $\sqrt{s} = 1.8$ TeV.

ACKNOWLEDGMENTS

Stimulating discussions with T. Stanev, R. Engel, D. Heck, J. Knapp, S. S. Ostapchenco and M. M. Block are gratefully acknowledged.

[1] R. J. Glauber and G. Matthiae, Nucl. Phys. **B21**, 135 (1970).
[2] R. Engel, T. K. Gaisser, and T. Stanev, Phys. Rev. D **58**, 014019 (1998).
[3] T. K. Gaisser, U. P. Sukhatme, and G. B. Yodh, Phys. Rev. D **36**, 1350 (1987).
[4] L. Durand and H. Pi, Phys. Rev. D **38**, 78 (1988).
[5] B. Z. Kopeliovich, B. Z. Nikolaev, and I. K. Potashnikova, Phys. Rev. D **39**, 769 (1989).
[6] M. M. Block, F. Halzen, and T. Stanev, Phys. Rev. Lett. **83**, 4926 (1999).
[7] M. M. Block, F. Halzen, and T. Stanev, Phys. Rev. D **62**, 077501 (2000).
[8] M. M. Block, Phys. Rep. **436**, 71 (2006).
[9] J. Bellandi *et al.*, Phys. Lett. B **343**, 410 (1995).
[10] F. Abe *et al.*, Phys. Rev. D **50**, 5550 (1994).
[11] N. A. Amos *et al.*, Phys. Lett. B **243**, 158 (1990).
[12] C. Avila *et al.*, Phys. Lett. B **445**, 419 (1999).
[13] M. Aglietta *et al.*, Astropart. Phys. **10**, 1 (1999).
[14] M. Aglietta *et al.*, Astropart. Phys. **21**, 583 (2004).
[15] T. Antoni *et al.*, Astropart. Phys. **24**, 1 (2005).
[16] T. Hara *et al.*, Phys. Rev. Lett. **50**, 2058 (1983).
[17] M. Honda *et al.*, Phys. Rev. Lett. **70**, 525 (1993).
[18] M. Aglietta *et al.*, Nucl. Phys. B, Proc. Suppl. **75**, 222 (1999); in *Proceedings of the 30th International Cosmic Ray Conference, Merida, Yucatan, Mexico, 2007*, edited by R. Caballero, J. C. D'Olivo, G. Medina-Tanco, L. Nellen, F. A. Sánchez, and J. F. Valdés-Galicia

(Universidad Nacional Autónoma de México, Mexico City, Mexico, 2008), Vol. 4, p. 27.
[19] R. M. Baltrusaitis *et al.*, Phys. Rev. Lett. **52**, 1380 (1984).
[20] K. Belov *et al.*, Nucl. Phys. B, Proc. Suppl. **151**, 197 (2006).
[21] K. Kamata and J. Nishimura, Prog. Theor. Phys. Suppl. **6**, 93 (1958).
[22] M. Aglietta *et al.*, Nucl. Instrum. Methods Phys. Res., Sect. A **336**, 310 (1993).
[23] D. Heck *et al.*, Forschungszentrum Karlsruhe Report No. FZKA 6019, 1998.
[24] S. Ostapchenko, Phys. Rev. D **74**, 014026 (2006).
[25] R. Engel *et al.*, in *Proceedings of the 26th International Cosmic Ray Conference, Salt Lake City, Utah, USA, 1999*, edited by B. L. Dingus, D. B. Kieda, and M. H. Salomon (AIP, Melville, NY, 2000), Vol. 1, p. 415.
[26] H. Fesefeldt, RWTH, Aachen Report No. PITHA-85/02, 1985.
[27] K. Greisen, Annu. Rev. Nucl. Sci. **10**, 63 (1960).
[28] T. Antoni *et al.*, Astropart. Phys. **24**, 467 (2006).
[29] R. Brun and F. Carminati, CERN Program Library Long Writeup W5013, 1994.
[30] J. N. Capdevielle, J. Phys. G **15**, 909 (1989).
[31] J. R. Hörandel, J. Phys. G **29**, 2439 (2003).
[32] H. H. Mielke, J. Phys. G **20**, 637 (1994).
[33] G. B. Yodh, S. C. Tonwar, T. K. Gaisser, and R. W. Ellsworth, Phys. Rev. D **27**, 1183 (1983).
[34] I. De Mitri *et al.*, in *Proceedings of the 30th International Cosmic Ray Conference, Merida, Yucatan, Mexico, 2007*, edited by R. Caballero, J. C. D'Olivo, G. Medina-Tanco, L. Nellen, F. A. Sánchez, and J. F. Valdés-Galicia (Universidad Nacional Autónoma de México, Mexico City, Mexico, 2008), Vol. 4, p. 675.
[35] K. Werner, F. M. Liu, and T. Pierog, Phys. Rev. C **74**, 044902 (2006).